

Near Mean Motion Resonance of Terrestrial Planet Pair Induced by Giant Planet: Application to Kepler-68 System

Mengrui Pan,^{1,2} Su Wang,^{1*} Jianghui Ji^{1,2,3†}

¹CAS Key Laboratory of Planetary Sciences, Purple Mountain Observatory, Chinese Academy of Sciences, Nanjing 210008, China

²School of Astronomy and Space Science, University of Science and Technology of China, Hefei 230026, China

³CAS Center for Excellence in Comparative Planetology, Hefei 230026, China

26 June 2020

ABSTRACT

In this work, we investigate configuration formation of two inner terrestrial planets near mean motion resonance (MMRs) induced by the perturbation of a distant gas-giant for the Kepler-68 system, by conducting thousands of numerical simulations. The results show that the formation of terrestrial planets is relevant to the speed of Type I migration, the mass of planets, and the existence of giant planet. The mass and eccentricity of the giant planet may play a crucial role in shaping the final configuration of the system. The inner planet pair can be trapped in 5:3 or 7:4 MMRs if the giant planet revolves the central star with an eccentric orbit, which is similar to the observed configuration of Kepler-68. Moreover, we find that the eccentricity of the middle planet can be excited to roughly 0.2 if the giant planet is more massive than 5 M_J , otherwise the terrestrial planets are inclined to remain near-circular orbits. Our study may provide a likely formation scenario for the planetary systems that harbor several terrestrial planets near MMRs inside and one gas-giant exterior to them.

Key words: planetary systems – methods: numerical – planets and satellites: formation.

1 INTRODUCTION

Kepler space telescope discovered a great number of tightly packed terrestrial planet pairs, which are involved in or near mean motion resonances (MMRs) (Lissauer et al. 2011a; Ford et al. 2012; Rowe et al. 2014; Gozdziewski et al. 2016; Berger et al. 2018). From a viewpoint of statistics, for Kepler planetary candidates, there are two peaks at the distribution of period ratio of two adjacent terrestrial planets near 1.5 and 2.0, respectively (Lissauer et al. 2011b; Fabrycky et al. 2014; Gillon et al. 2017; Charalambous et al. 2018). Figure 1 shows the distribution of period ratios of adjacent terrestrial planet pairs whose masses are confirmed (Herein we refer to the terrestrial planet with a mass $M_p < 10 M_\oplus$), where 87 terrestrial planet pairs are included. Most of them locate close to central star. The entire distribution of period ratios illustrates that the planet pairs have a pileup around 5:3, 3:2, 2:1, 5:2 and 3:1 MMRs. Combined with abundant observations, the near-resonant terrestrial planet pairs, accompanied by one or more gas-giants, are also discovered in a couple of planetary systems, e.g., Kepler-48, Kepler-68 and Kepler-154

(Marcy et al. 2014; Uehara et al. 2016; Mills et al. 2019). Thus, this leads to the crucial questions: what scenario may produce the configuration of terrestrial planet pairs near MMRs, and how the formation of such configuration can be affected if there exists an additional gas-giant exterior to the terrestrial planet pair?

Several scenarios, such as in situ formation (Chiang & Laughlin 2013), inside-out formation (Chatterjee & Tan 2014), pebble-accretion (Liu & Ormel 2018; Liu et al. 2019), or late orbital instability after disk depletion (Izidoro et al. 2017; Ogihara et al. 2018; Lambrechts et al. 2019) have been suggested to explain the formation of hot super-Earth in or near MMR configuration. However, Ogihara et al. (2015) claimed close-in super-Earths cannot be formed in situ, unless their migration speed is suppressed in the entire disk inside 1 AU. The widely-accepted theory indicates that the short-period planets are formed at large distance far away from their host stars and migrate to currently observed orbits through angular momentum exchange with protoplanetary disk (Lin & Papaloizou 1986; Ward 1997; Raymond et al. 2018). A large majority of planets in compacted systems are super-Earths that can be easily trapped into MMRs through Type I migration (Cresswell & Nelson 2006).

*

† E-mail: jijh@pmo.ac.cn, wangsu@pmo.ac.cn

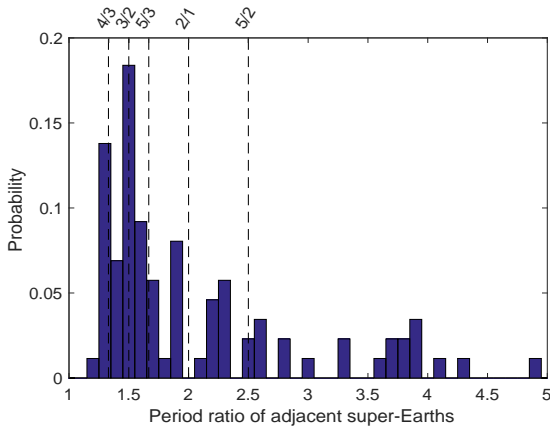


Figure 1. Distribution of period ratio of two adjacent super-Earths in exoplanetary systems.

In addition, previous studies proposed an alternative scenario to shed light on the formation of near-resonant systems via Type I migration (Wang, Ji & Zhou 2012; Wang & Ji 2014, 2017). As a matter of fact, most of the confirmed planet pairs are not trapped in exact MMRs. The stellar magnetic field, inviscid disks or turbulence in protoplanetary disk triggered by magneto-rotational instability stochastic can reproduce the distribution of period ratio bearing resemblance to nowadays observations of the planet pair (Rein 2012; Paardekooper et al. 2013; Liu & Ormel 2017; McNally et al. 2019; Liu et al. 2019). Other mechanism suggests that planet-planet scattering and final mergers of several core/planets in the cavity tend to disrupt the MMRs established during the migration (Terquem & Papaloizou 2007). Furthermore, for those systems that tidal dissipation is unexpectedly efficient, weak dissipation damps the eccentricities of planets, thereby driving the near-resonant pairs move out of resonance (Lithwick & Wu 2012; Lee et al. 2013). In summary, the above scenarios give some explanations on the formation of system with terrestrial planets.

So far, a large number of systems, which host giant planets involved in MMRs, have been extensively investigated (Lee & Peale 2002; Robertson et al. 2012; Lee et al. 2013; Marti et al. 2013; Wittenmyer et al. 2016; Marti et al. 2016; Bae et al. 2019). Figure 1 contains nine systems with the co-existence of terrestrial planets and gas-giant (with a mass above $0.1 M_J$). The planetary embryos can be accelerated to collide and merge into terrestrial cores, further to produce super-Earth size, close-in terrestrial planets under the circumstance of an additional gas-giant in the system (Zhou et al. 2005; Raymond et al. 2006; Mandell et al. 2007; Hands & Alexander 2016; Sun et al. 2017). For instance, Hands & Alexander (2016) suggested the outer planet, which can undergo exponential growth up into a giant planet, tends to push interior super-Earths into more tightly first-order resonant orbits. Sun et al. (2017) revealed that MMRs configuration can occur between gas-giants and terrestrial planets. Granados et al. (2018) showed that an undetected outer giant planet may have an effect on the stability and resultant configuration of tightly packed inner

planets by secular resonance. Therefore, we believe that the existence of giant planet, in fact, does play a significant role in sculpting final configuration of the system.

The objective of the present work is to study the influence of a faraway gas-giant on the configuration formation of terrestrial planets especially for the planet pair in or near MMRs. Here we take Kepler-68 system as a template, which consists of two inner terrestrial planets involved in near MMRs and a distant giant companion (Gilliland et al. 2013; Stassun et al. 2017). Kepler-68 is a solar-mass ($\sim 1.08 M_\odot$) star with effective temperature ~ 5793 K (Gilliland et al. 2013; Stassun et al. 2017). Two transiting Earth-sized planets were discovered around the star at a distance of 0.0617 and 0.09059 AU, respectively. The period ratio of the inner planet pair is roughly 1.779, which is between 1.5 and 2.0. An additional Jupiter-mass planet, which locates exterior to two terrestrial planets at 1.4 AU, was detected by radial velocity (Gilliland et al. 2013; Marcy et al. 2014) (see Table 1). Consequently, this enables us to improve the understanding of formation of near-resonant terrestrial planets.

One of the most noteworthy is the eccentricities of Kepler-68 b and c. They were constrained to be zero by modelling (Gilliland et al. 2013; Mills et al. 2019), while Van Eylen & Albrecht (2015) pointed out that the eccentricity of Kepler-68 c could amount up to 0.42 based on high-quality Kepler transit observations, which can remain steady for 10^8 years in the simulation.

The formation scenario of late orbital instability may be one of possible mechanism to explain the formation of the inner configuration of two terrestrial planets (Izidoro et al. 2017; Ogihara et al. 2018; Lambrechts et al. 2019). After the late orbital instability, the typical orbital separation between planets is about $20 R_H$, which is comparable to the current orbital separation between Pb and Pc in the Kepler-68 system. In addition, as the period ratio of Pb and Pc is 1.78, which is out of the exact 5:3 resonance by more than 5%, this system can be regarded as a non-resonant system. The late orbital instability can explain the formation of non-resonant systems. Furthermore, the eccentricity of Pc can be excited to some extent during the late orbital instability. In consideration of the existence of giant planet in the outer region, here we aim to figure out the configuration formation of the inner planet pair, and further investigate the excitation of eccentricity of the middle planet under the influence of a giant planet lying outside in Kepler-68 system. In this work, the inner planet pair can be trapped in 5:3 or 7:4 MMRs if the giant planet moves around the central star in an eccentric orbit, which is similar to the observed orbits, deviating from the exact 2:1 or 3:2 MMRs. Moreover, we find that if the giant planet is more massive than $5 M_J$, the eccentricity of the middle planet can be excited to approximately 0.2.

This paper is organized as follows. In Section 2, we present the gas disk model and Type I migration scenario adopted in our simulations. In Section 3, we show the numerical simulation results with respect to the Kepler-68 system. We summarize major conclusions in Section 4.

Table 1. Orbital Parameters of the Kepler-68 Planetary System.

Planet	Mass (M_{\oplus})	Semi-major axis (AU)	Eccentricity		Orbital Period (day)
			(1)	(2)	
b	$5.98^{+1.70}_{-1.70}$	$0.0617^{+0.00056}_{-0.00056}$	0.0	$0.02^{+0.13}_{-0.02}$	$5.399^{+0.000004}_{-0.000004}$
c	$2.18^{+0.011}_{-0.011}$	$0.09059^{+0.00082}_{-0.00082}$	0.0	$0.42^{+0.41}_{-0.1}$	$9.605^{+0.000072}_{-0.000072}$
d	$308.5^{+11.124}_{-11.124}$	$1.4^{+0.03}_{-0.03}$	$0.18^{+0.05}_{-0.05}$	-	580^{+15}_{-15}

Note: The parameters are adopted from <https://exoplanetarchive.ipac.caltech.edu/index.html>, Gilliland et al. (2013), Mills et al. (2019), Van Eylen & Albrecht (2015).

2 MODELS

2.1 Disk models

To explore the configuration formation of Kepler-68 system, we make an assumption that planets are formed in the protoplanetary disks. Here we take empirical Minimum-Mass Solar Nebular (MMSN) model (Hayashi 1981) as the gas disk model. Thus the density at a stellar distance a can be described as follows

$$\Sigma_g = \Sigma_0 \left(\frac{a}{1 \text{ AU}} \right)^{-k} \exp\left(-\frac{t}{t_n}\right), \quad (1)$$

where $\Sigma_0 = 1700 \text{ g cm}^{-2}$ is the initial density of the gas disk. The disk model can be shallower and the surface density can be larger or smaller than the classical model (Bitsch et al. 2015; Suzuki et al. 2016). In this paper, we mainly forced on the influence of the giant planet on the final configuration of the inner terrestrial planets. Considering that Kepler-68 is a solar-mass star, we regard as MMSN the power-law index of the gas disk density $k = 3/2$. t_n is the disk depletion timescale, which is observed to be approximately few million years (Haisch et al. 2001). In this work, we assume $t_n = 10^6$ yr. In the simulation, an inner hole of the gas disk occurs around the central star due to the star magnetic field, thus the gas disk is roughly truncated at the corotation radius of star about nine stellar radii (Koenigl 1991). The stellar radius would be 2-3 times larger before the protostar becomes a main sequence object. The radius of central star for Kepler-68 system is approximately $1.24 R_{\odot}$ (Batalha et al. 2013), consequently the inner boundary of the gas disk is at roughly 0.1-0.15 AU. With the evolution of central star, the truncation radius will decrease. It is possible that the truncation radius is smaller than 0.1-0.15 AU in the planet formation stage (Bouvier et al. 2014). Under such estimation, we set the inner edge of the gas cavity to be 0.1 AU.

2.2 Type I migration and eccentricity damping

For a planet embedded in a protoplanetary disk, the exchange of angular momentum between planet and gaseous disk will trigger orbital migration of planets. If the mass of the planet is not larger than $30 M_{\oplus}$, the variation of angular momentum on planets will give rise to type I migration (Tanaka et al. 2002; Papaloizou & Larwood 2000), the

timescale of Type I migration on planet with a mass m is given by

$$\begin{aligned} \tau_{\text{migI}} &= \frac{a}{|\dot{a}|} = \frac{1}{f_1} \tau_{\text{linear}} \\ &= \frac{1}{f_1 (2.7 + 1.1\beta)} \left(\frac{M_*}{m} \right) \left(\frac{M_*}{\Sigma_g a^2} \right) \left(\frac{h}{a} \right)^2 \\ &\quad \times \left[\frac{1 + \left(\frac{er}{1.3h} \right)^5}{1 - \left(\frac{er}{1.1h} \right)^4} \right] \Omega^{-1} \text{ yr}, \end{aligned} \quad (2)$$

where τ_{linear} is the linear analysis result and f_1 is a reduction factor of migration speed. In our simulations, we suppose f_1 ranging from 0.1 to 1. β is the coefficient and $\beta = -d \ln \Sigma_g / d \ln a$. M_* is the mass of central star and $\Omega = \sqrt{GM_*/r^3}$ presents Keplerian angular velocity. h , r , a , e and m are scale height of disk, distance between planet and star, semi-major axis, eccentricity and mass of planet, respectively. Considering the disk model we used, the timescale of Type II migration is much longer than that of Type I migration (Duffell et al. 2014; Dürmann & Kley 2015), the movement of giant planet could be negligible (Baruteau et al. 2014). Here we ignore Type II migration of Planet d.

In addition, planet-disk interaction results in damping of orbital eccentricity over a timescale of (Cresswell & Nelson 2006)

$$\begin{aligned} \tau_e &= \left(\frac{e}{\dot{e}} \right)_{\text{edamp}} \\ &= \frac{Q_e}{0.78} \left(\frac{M_*}{m} \right) \left(\frac{M_*}{a^2 \Sigma_g} \right) \left(\frac{h}{r} \right)^4 \Omega^{-1} \left[1 + \frac{1}{4} \left(\frac{er}{h} \right)^3 \right] \text{ yr}, \end{aligned} \quad (3)$$

where Q_e is a normalization factor and here we adopt $Q_e = 0.1$. Other symbols are the same as in Equation 2. Orbital migration and eccentricity damping, induced by the gas disk, will diminish when the planet enters into the inner hole.

3 NUMERICAL SIMULATION RESULTS

To explore the configuration formation of Kepler-68 planetary system, we assume two terrestrial planets are originally born far away from their nominal locations, and then undergo type I migration caused by the gas disk, along with a settled outermost gas-giant. Therefore, the acceleration of the terrestrial planet with m_i is expressed as

$$\frac{d}{dt}\mathbf{V}_i = -\frac{G(M_* + m_i)}{r_i^2} \left(\frac{\mathbf{r}_i}{r_i} \right) + \sum_{j \neq i}^N Gm_j \left[\frac{(\mathbf{r}_j - \mathbf{r}_i)}{|\mathbf{r}_j - \mathbf{r}_i|^3} - \frac{\mathbf{r}_j}{r_j^3} \right] + \mathbf{F}_{\text{damp}} + \mathbf{F}_{\text{migI}}, \quad (4)$$

where

$$\mathbf{F}_{\text{damp}} = -2 \frac{(\mathbf{V}_i \cdot \mathbf{r}_i) \mathbf{r}_i}{r_i^2 \tau_e}, \quad (5)$$

$$\mathbf{F}_{\text{migI}} = -\frac{\mathbf{V}_i}{2\tau_{\text{migI}}}.$$

For the gas-giant, we only consider the gravitational interaction with other planets and the central star. To simulate the orbital evolution of each planet, we have modified N-body integrator of MERCURY6 (Chambers 1999). In our simulations, the time step for each integration is set to be less than 1/50 of orbital period of the innermost planet and the integration accuracy is 10^{-15} . The argument of pericenter, longitude of ascending node and mean anomaly (hereafter the three angles) of planets are randomly generated between 0° and 360° . The eccentricities are initially assumed to be zero and all planets are supposed to be co-planar.

In this work, we have performed 1610 runs in total, with an integration timescale ranging from 0.25-2 Myrs, depending on the system stability and planetary migration rate. It is possible that there are more than two terrestrial planets in the systems. In this paper, we mainly focused on studying the influence on the configuration between the confirmed planets. Considering other possible existed terrestrial planets is not massive enough to influence the final configuration of planet b and c, we only assume that there are two terrestrial planets in the system. §3.1 shows the results of the the systems composed of only two terrestrial planets for Group 1, whereas in §3.2, we investigate the formation of the inner terrestrial planets affected by the giant planet for Group 2. For all runs, we label the innermost planet as P_b and the middle planet as P_c , where the subscripts b and c denote each of them, respectively, while P_d represents the outermost companion in the system.

3.1 Group 1: Terrestrial planets migrate without giant planet

In this Section, we carry out a series of simulations using a wide variety of initial positions of P_b and P_c , to examine configuration formation for the terrestrial planet pair without the presence of the giant planet in the Kepler-68 system. The contribution of disk to planets is described as in Equation (2) and (3). We let $f_1 = 0.1, 0.3, 0.5, 0.8$ and 1, respectively. Considering the currently observed semi-major axis of P_d and the inner edge of gaseous disk. According to Kokubo & Ida (1998), after oligarchic growth, the orbital separations between planets are wider than 5 Hill radius, and the typical orbital separation is about 10 Hill radius. Based on Zhou et al. (2007), the stable time for the planets with few earth-mass is larger than 10^5 years when the separation between them is larger than 5 Hill radius. And according to the estimation of Ford et al. (2001), planetary system would maintain stable if their relative orbital separation is larger than 3.5 Hill radius. Therefore, in this work, we set the initial location of P_b ranging from 0.2 to 1.2 AU, whereas that

of P_c spans from 0.3 to 1.3 AU with an equally-spaced separation of 0.1 AU which makes the initial separation between two terrestrial planets larger than 3.5 Hill radius. Then we have performed 66 simulations for each f_1 by means of the initials of P_b and P_c . Thus we entirely implement 330 runs.

From the numerical outcomes, we find that the initial position of planets and their mutual separation actually have no remarkable influence on the final configuration of the planetary system. However, the speed of type I migration plays a key role in affecting the final configuration of the planet pair. For $0.3 \leq f_1 \leq 1$, Kepler-68 b and c prefer to be captured into 3:2 MMR, whereas for $f_1 = 0.1$, planets with lower migration speed are trapped into 2:1 MMR rather than 3:2 MMR. These results are consistent with those of Wang, Ji & Zhou (2012). The typical evolution for the cases is shown in Figure 2 for $f_1 = 0.1$ and $f_1 = 0.3$, respectively. The major initial conditions and the final results are shown in G1-1 and G1-2 of Table 2. Planet b and c are assumed to start migrating from 0.5 and 1 AU for two cases, respectively. Solid lines illustrate the results of $f_1 = 0.1$, while the dashed blue and red lines display those outcomes of $f_1 = 0.3$. The gray lines indicate the nominal locations of two terrestrial planets in the system. As shown in Figure 2, without a remarkable reduction in the speed of migration, the terrestrial planets are quickly locked into 3:2 MMR at about 0.03 Myr, while for a lower migration speed, the planets are trapped into 2:1 MMR at about 1.2 Myr. The final eccentricity of planet c is a bit higher than planet b in G1-2, as compared with that of G1-1.

As planet b is more massive than planet c, P_b always migrates faster than P_c according to the timescale of type I migration given in Equation (2) before they arrive at the inner edge of gas disk. Once P_b reaches the inner boundary of gas disk, the planet will halt migrating because of the absence of gas. When P_c approaches P_b , the two terrestrial planets will be captured into resonance and the planet pair will migrate in the same pattern until P_c stops migration near the inner edge of gas disk. Based on our estimation, the inner boundary of the gas disk locates at about 0.1 AU, which is very close to the observed orbit of P_c . Thus, through type I migration from outside, P_c can be formed near its nominal location. If the inner boundary of gas disk locates closer than 0.1 AU (Bouvier et al. 2014), the final location of P_c may change as the inner disk edge moves much closer to the star. Therefore, the location of disk edge suggests that terrestrial planets may have been born at the early stage of the central star that the truncation radius is around 0.1 AU according to our estimation.

In our simulations, we find that 80% of planet pairs are trapped in 3:2 MMRs, whereas 20% of planet pairs are involved in 2:1 MMRs at the end of runs. The simulations indicate that the planet pairs are entirely trapped into first-order MMRs concerning with a wide variety of initial region and speed of type I migration. The resultant orbital periods of P_c is approximately 10 days, while that of P_b is observed to be either 5.45 or 6.84 days, depending on what kinds of MMRs they enter into. If there are additional terrestrial planets migrating toward the proximity of the inner two terrestrial planets, the final configuration of inner planet pair is similar to the results as shown in Group 1, but it will increase possibility of planet pair involved in more compact configuration. For the systems that are composed of three

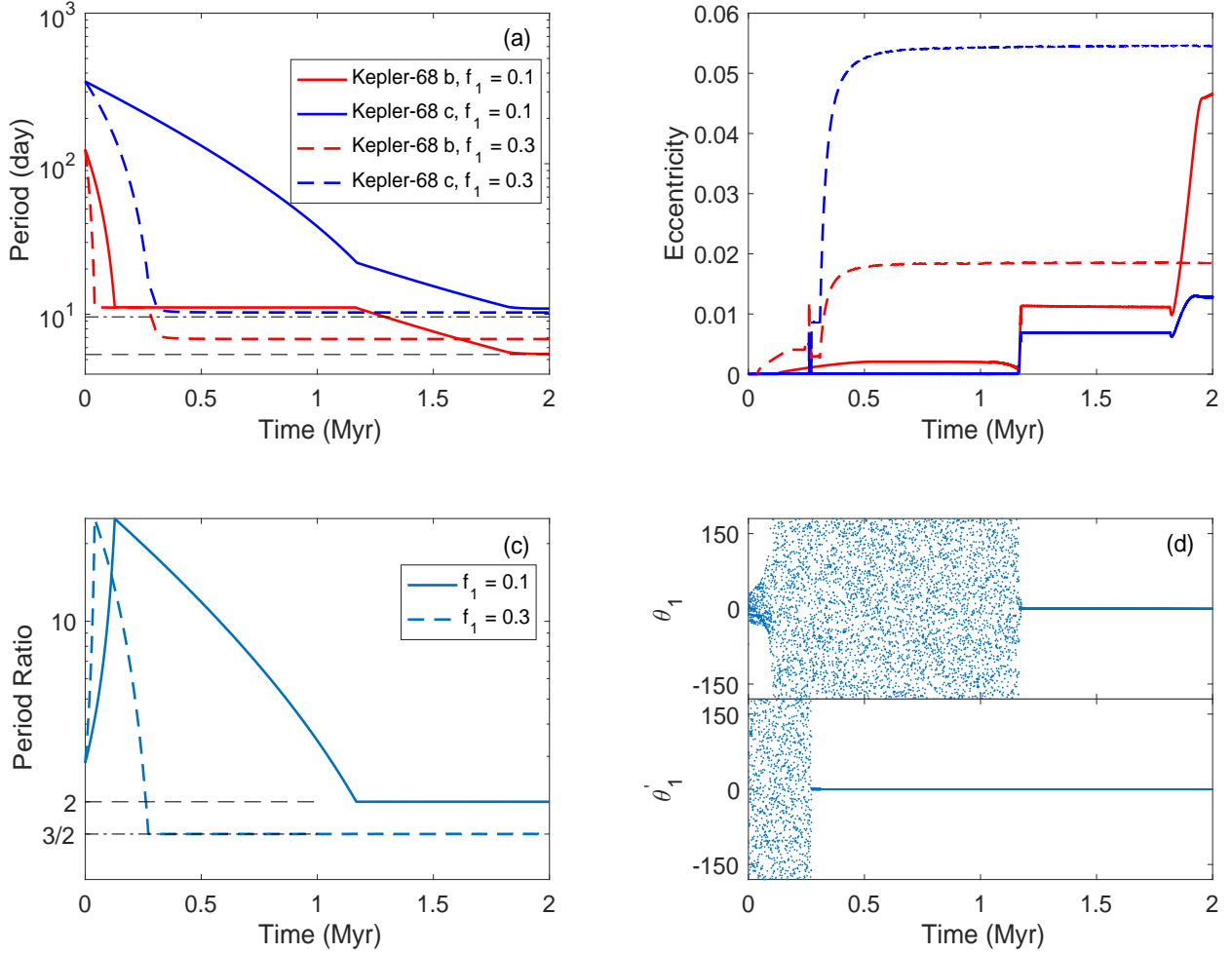


Figure 2. Orbital evolution of G1-1 and G1-2. Solid lines represent the run with $f_1 = 0.1$ (G1-1), whereas the dashed lines for $f_1 = 0.3$ (G1-2). The initial locations of P_b and P_c are at 0.5 and 1 AU, respectively. Panel (a), (b), (c) and (d) show the evolution of orbital period, eccentricity, period ratio, and resonant angle, respectively. In Panel (a), the dashed and dash-dotted lines (in gray), respectively, illustrate the currently observed orbital period of Kepler-68 b and Kepler-68 c. Red and blue lines of two upper Panels, respectively, display the orbital period and eccentricity against the time over 2 Myrs for two planets. P_b and P_c are trapped in 2:1 MMR for $f_1 = 0.1$, while captured in 3:2 MMR for $f_1 = 0.3$. Panel (d) provides the time variation of the resonant angles $\theta_1 = \lambda_1 - 2\lambda_2 + \varpi_1$ of 2:1 MMR and $\theta'_1 = 2\lambda_1 - 3\lambda_2 + \varpi_1$ of 3:2 MMR, which librate slightly about 0° when they enter into each MMR.

Table 2. Parameters adopted in our simulations for G1 and G2.

Case No.	p_{b0} (day)	p_{c0} (day)	f_1	p_{bf} (day)	p_{cf} (day)	e_{bf}	e_{cf}	Giant Planet	p_{d0} (day)	e_{d0}	m_d (M_J)
G1-1	124	352	0.1	5.453	10.91	0.047	0.013	N	-	-	-
G1-2	124	352	0.3	6.844	10.27	0.019	0.055	N	-	-	-
G2-1	124	352	0.1	5.448	10.9	0.053	0.012	Y	580	0.0	0.97
G2-2	124	352	0.3	6.844	10.27	0.019	0.055	Y	580	0.0	0.97
G2-3	312	261	0.8	6.844	10.27	0.055	0.019	Y	580	0.0	0.97
G2-4	124	352	0.3	6.17	10.28	0.0165	0.053	Y	580	0.18	0.97
G2-5	33	60	0.1	6.111	10.69	0.033 ± 0.0046	0.0138 ± 0.013	Y	129	0.03	10.0

Note: p_{b0} and p_{c0} , respectively, represent the initial orbital period of P_b and P_c , while p_{bf} and p_{cf} stand for each of the final period. e_{bf} and e_{cf} denote each of the final eccentricity. p_{d0} , e_{d0} , and m_d represent the initial orbital period, eccentricity, and mass of P_d .

terrestrial planets, the planet pairs have more opportunity to be in 3:2 MMR (Wang & Ji 2014, 2017) in the migration scenario. Therefore, here our primary goal is to investigate how the configuration of inner planet pair is affected by a distant gas-giant in the system for only two terrestrial planets formed.

Here we choose G1-1 and G1-2 as two typical models to examine the situation of formation of inner planet pair affected by the outermost giant planet. Using similar initial parameters of G1-1 and G1-2, we then carry out 100 simulations for each f_1 . The simulations reveal that the planet pairs are entirely trapped into 2:1 MMR for $f_1 = 0.1$, whereas they are associated with 3:2 MMR for $f_1 = 0.3$. These results agree with those of G1-1 and G1-2. According to equation (2), the timescale of type I migration is proportional to $(mr)^{-1}$. The masses of inner terrestrial planets in the system is 5.98 and 2.18 M_\oplus . Based on these initial settings, the speed of type I migration of the innermost planet is higher than the second terrestrial planet initially. The innermost planet migrate to the inner edge first and then the second one catch up with the innermost planet around the disk edge. Therefore, the relative speed between two terrestrial planets is not so high leading to the capture of 2:1 and 3:2 MMRs rather than 4:3 MMR (Mustill & Wyatt 2011; Ogihara & Kobayashi 2013).

3.2 Group 2: Terrestrial planets migrate with perturbation of giant planet

In Kepler-68 system, Gilliland et al. (2013) showed that the additional giant planet locates at about 1.4 AU, which is far away from the nominal regime of terrestrial planets. In such circumstance, the formation of inner terrestrial planets P_b and P_c would be influenced due to the existence of the gas-giant. Some study suggests that the giant planets can be formed in the system earlier than the terrestrial planets (Lykawka & Ito 2013). Thus, in Group 2, we assume the giant planet P_d first occurred in the outer region compared with the two inner companions, and we will extensively investigate the migration of the inner planets induced by the perturbation of giant planet in the system. To further clarify this issue, here we perform more simulations of three subgroups based on the orbital period and eccentricity of P_d . In the following, we will present the detailed exploration.

Subgroup 1: P_d initially locates on circular orbit at 1.4 AU. Same as in Group 1, 330 runs are performed using various initial locations of two terrestrial planets, and other 200 cases are run for planet b and c at 0.5 and 1 AU, respectively, for $f_1 = 0.1$ and $f_1 = 0.3$, respectively.

Subgroup 2: P_d originally moves on an eccentric orbit of $e_d = 0.18$ at 1.4 AU, whereas P_b and P_c reside at 0.5 and 1.0 AU, respectively, at the beginning of simulations. Here we adopt $f_1 = 0.1$ and $f_1 = 0.3$. And we run 200 simulations.

Subgroup 3: P_b and P_c locate at 0.2 and 0.3 AU initially. We adopt $f_1 = 0.1$ and $f_1 = 0.3$, respectively. To explore the formation of two terrestrial planets influenced by the gas-giant on circular orbits, we perform 150 runs with a family of combined parameter of m_d of 1, 5, and 10 M_J , a_d ranging from 0.4 to 0.8 AU. As a comparison, we then carry out 200 additional runs in the case that P_d moves on eccentric orbits at 0.5 AU for $e_d = 0.03$ and $e_d = 0.1$, respectively.

3.2.1 Subgroup 1: Giant planet on circular orbit formed at its nominal location

First of all, we consider similar cases as in §3.1, but with an additional giant planet P_d lying beyond P_b and P_c on a circular orbit. The initial mass and semi-major axis of P_d in the simulations are the observed values as given in Table 1.

Among 330 cases, 24% of unstable systems in the results are induced by the small separation which is near the boundary of 3.5 R_H . In this section, we mainly discuss the results of 250 stable cases.

Figure 3 shows the dynamical evolution of two typical stable cases. To compare with the results in Group 1, we adopt the same initial parameters of G2-1 and G2-2 as those of G1-1 and G1-2. However, to better understand how the configuration of two terrestrial planets is affected, in the simulations we add the perturbation arising from the giant planet with a circular orbit. Panel (b) of Figure 3 exhibits the eccentricity of P_c is excited to about 0.1 at the very beginning. However, as the planet interacts with the gas disk, the excited eccentricity can go down to near zero very quickly. In the meantime, the semi-major axis of planets decreases due to angular momentum conservation. Clearly, it is easy to note that the migration speed of P_c in G2-1 and G2-2 is faster than that in Group 1. Panel (d) shows the resonant angles $\theta_1 = \lambda_1 - 2\lambda_2 + \varpi_1$ of 2:1 MMR and $\theta'_1 = 2\lambda_1 - 3\lambda_2 + \varpi_1$ of 3:2 MMR librate slightly about 0° when two inner terrestrial planets are captured into each MMR. Although there exists a giant planet, the configuration of the terrestrial planet pair is not changed for this group.

When planets move inward, the eccentricities of P_b and P_c can be excited for several times as they approach to the gas-giant. In the evolution, terrestrial planets have opportunities to exchange their orbits. The excitation always happens at the earlier evolution of simulations, the gas disk still remains dense enough to damp the eccentricity. Thus, the system can retain stable after the orbital exchange. Here we come to conclusion that the systems like Kepler-68 might have undergone orbital exchange. According to the estimation of isolation mass, the mass of solid core is proportional to $a^{3/4}$ (Ida & Lin 2004). In Kepler-68 system, P_b is more massive than P_c . They may exchange their orbits once. Figure 4 shows the evolution of a typical case that P_b and P_c locate at 0.9 and 0.8 AU, respectively. The starting conditions are denoted by G2-3 in Table 2. They migrate with $f_1 = 0.8$. P_d , moving on circular orbit, originally resides at 1.4 AU. The eccentricity of P_b and P_c can be frequently excited to about 0.1 and decline to near zero within a shorter timescale because of the disk. Orbital exchange occurs at about a few hundred years. The subsequent evolution of two terrestrial planets bears a resemblance to that of G2-1 and G2-2. Consequently, the inner planet pair is trapped into 3:2 MMR, which coincides with that of G2-2. Although the orbital exchange happened in case G2-3, there is only one case in this group, the possibility is about 0.4%. Additionally, the initial orbital separation of P_b and P_c is $\sim 6 R_H$. As the growth is faster for the inner planet, it is likely that the inner planet starts inward migration before the outer planet completes the growth. The orbital separation between two terrestrial planets tends to be larger. Considering the initial conditions and the possibility in this case, such orbital exchange may hardly occur, except for some particular conditions.

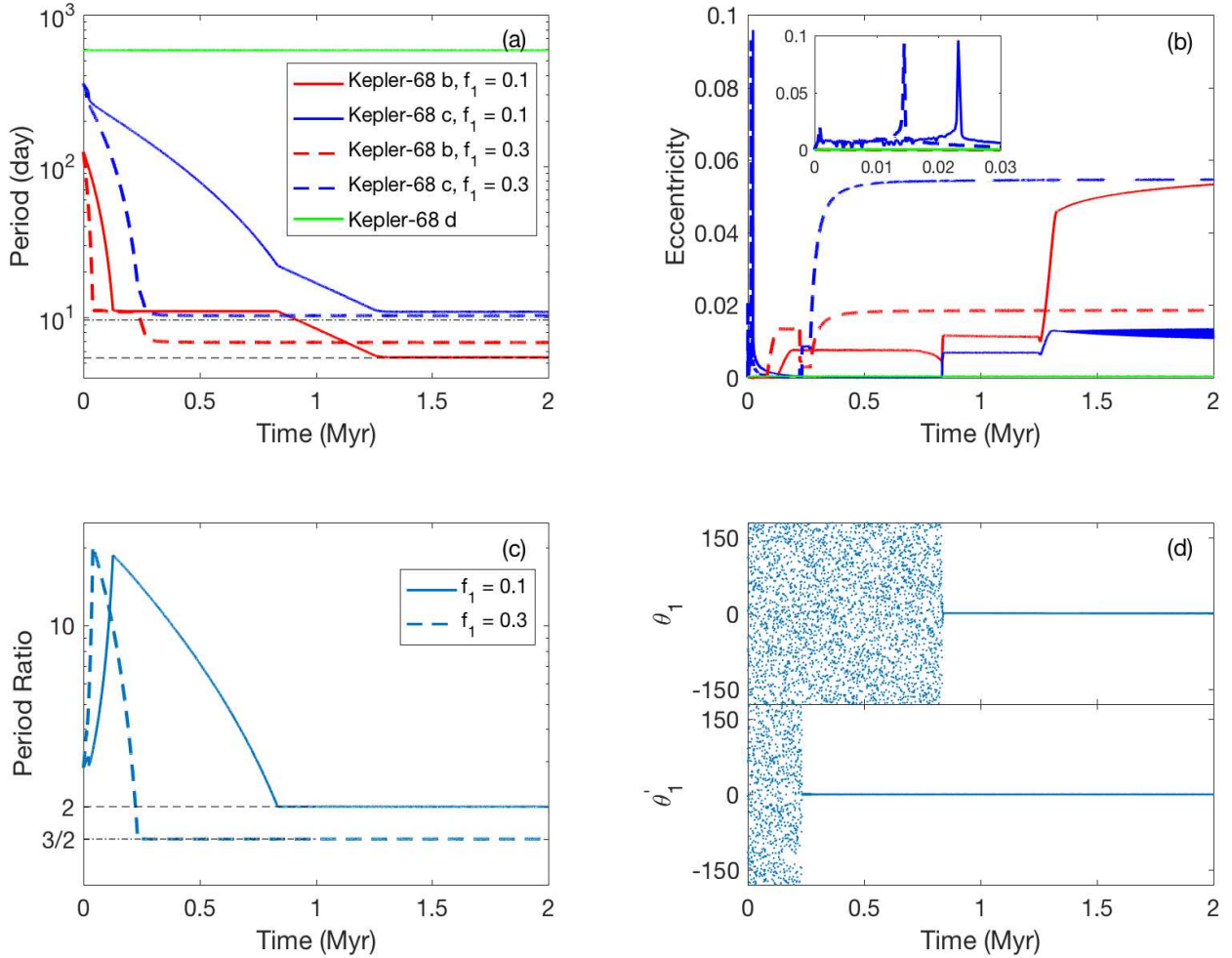


Figure 3. Same as in Figure 2, orbital evolution of G2-1 and G2-2. A giant planet d (by green line) initially orbit at 1.4 AU with $e_d = 0$. Panel (b) exhibits that the eccentricity of Kepler-68 c is excited by the giant planet at the early stage of migration but damped rapidly due to the disk. The giant planet can speed up the migration of two inner terrestrial planets. Panel (d) shows the resonant angles $\theta_1 = \lambda_1 - 2\lambda_2 + \varpi_1$ of 2:1 MMR and $\theta'_1 = 2\lambda_1 - 3\lambda_2 + \varpi_1$ of 3:2 MMR fluctuate slightly about 0° when two inner terrestrial planets are captured into each MMR.

With a giant planet on circular orbit at its nominal location, if terrestrial planet moves so close to P_d , the separation between them satisfies $\Delta \leq 0.2$ AU, then the system becomes unstable. If the terrestrial planet is close to P_d and suffer fast migration, orbital exchange can take place between two inner planets. Although the gas-giant can speed up migration rate of two terrestrial planets, it has no direct influence on resultant configuration of inner planet pair. Furthermore, we conduct 200 runs to examine this using similar parameters like those of G2-1 and G2-2, along with the variable three angles of planets. We find that the outcomes are consistent with those of G2-1 and G2-2.

3.2.2 Subgroup 2: Giant planet on eccentric orbit formed at its nominal location

As shown in Table 1, P_d is reported to be on eccentric orbit with $e_d = 0.18 \pm 0.05$. It is possible that P_d has already got its nominal eccentricity before the formation process of the inner terrestrial planets. Here we further study the configuration formation of inner terrestrial pair due to the perturbation of a giant planet on eccentric orbit. Here P_d is assumed to be 1.4 AU with an initial eccentricity $e_d = 0.18$. The locations and eccentricities of P_b and P_c , and f_1 are chosen as those of G1-1 and G1-2. Thus we carry out 100 cases for $f_1 = 0.1$ and $f_1 = 0.3$, respectively.

The results show that $\sim 83\%$ and $\sim 82\%$ of the systems are unstable for $f_1 = 0.1$ and $f_1 = 0.3$, respectively. Here we are particularly interested in those of stable cases involved in MMRs. For $f_1 = 0.1$, there are 4% and 1% of the systems hosting two terrestrial planets locked in 2:1 and 3:1 MMR,

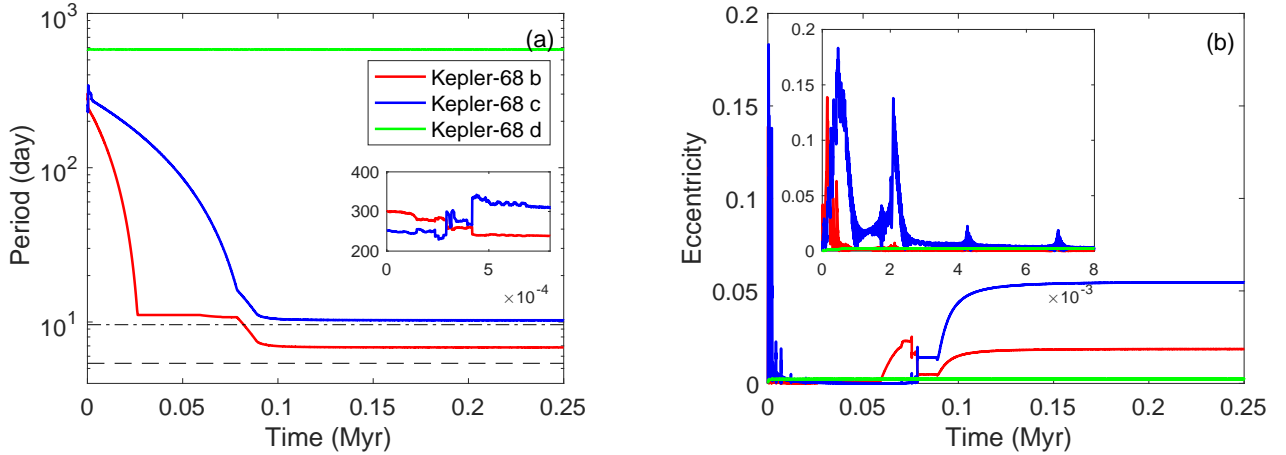


Figure 4. The evolution of G2-3. Panel (a) and (b) show the evolution of orbital periods and eccentricities, respectively. The zoomed window in Panel (a) displays that the two planets exchange their orbits at a very early stage with respect to the excitation of eccentricity in Panel (b). Note that the inner terrestrial pair can be trapped into 3:2 MMR in the evolution.

respectively. By contrast, 4%, 10% and 4% separately harbor the inner planet pair in 2:1, 3:2 and 5:3 MMRs for $f_1 = 0.3$.

Figure 5 illustrates the evolution of a typical run with two terrestrial planets in 5:3 MMR at the end of simulation. The initial conditions and final locations are displayed as G2-4 in Table 2. Here the eccentricity e_c of the middle planet is able to be excited up to 0.4 while e_b still remains a low value. In the simulations, both of P_c and P_d sustain eccentric orbits that may give rise to multiple orbit-crossing between them, thereby stirring e_c repetitively. From Panel (b) in Figure 5, we can see that e_c can be pumped up to above 0.3 within several thousand years. Subsequently, the migration speed of P_c increases all the time as a result of the damping of eccentricity induced by the gas disk, hence P_c arrives at the inner edge of gas disk in advance. However, we should emphasize that the inner planet pair can depart from 2:1 or 3:2 MMRs as P_c speeds up. As can be seen by Panel (d), P_c and P_b are tuned into 5:3 MMR, where the resonance angle $\theta_1 = 3\lambda_1 - 5\lambda_2 + 2\varpi_1$ librates about 180° for 1 Myr. This reminds us a very close configuration compared to the observed Kepler-68 system as reported in Table 1.

With a giant planet on eccentric orbit at its nominal location, a similar configuration can be produced through our formation scenario. If terrestrial planet formed at the outer region, which is quite close to the nominal location of giant planet, the eccentric orbit of giant planet will have influence on the nearby terrestrial planet impulsively leading to speeding up of the adjacent planet. In summary, we conclude that the inner terrestrial planet pair can be trapped into second-order MMR, which differs from the simulation results without a giant planet in the outer region.

3.2.3 Subgroup 3: Giant planet on eccentric orbit with different masses and semi-major axes

As aforementioned, the existence of P_d can affect the final configuration of the inner pair. Here we primarily aim to

study the circumstance for two terrestrial planets when P_d has a diverse mass and initial location.

First, we investigate dynamical evolution of the systems that harbor P_d on a circular orbit. In our simulations, we consider the initial parameters of the giant planet with a combined parameter of mass ($m_d = 1, 5, \text{ and } 10 M_J$), semi-major axes ($a_d = 0.4, 0.5, 0.6, 0.7, \text{ and } 0.8 \text{ AU}$), and the speed of type I migration ($f_1 = 0.1 \text{ and } 0.3$), then we perform 150 runs to explore how these parameters play a part in the evolution of the planets. The results reveal that the inner pair can be captured into 2:1 MMR for $f_1 = 0.1$ and 3:2 MMR for $f_1 = 0.3$, which is similar to those in Group 1.

Second, for P_d on eccentric orbit at 0.5 AU, P_b and P_c occupying the orbits at $a_b = 0.2$ and $a_c = 0.3$ AU, respectively, we carry out 200 simulations with respect to $e_d = 0.03$ and $e_d = 0.1$ for $f_1 = 0.1$. As mentioned above, the inner planet pair is involved in 2:1 MMR for $f_1 = 0.1$ in the case of without a gas-giant or with a giant planet on circular orbit. As a comparison, there is less than 15% of the runs trapped in 2:1 MMR for terrestrial planets. Moreover, approximately 50% of them turns to other MMRs.

For $e_d = 0.03$, we conduct 100 simulations. From the results, we find that 31% of the runs occupy two terrestrial planets involved in 3:2 MMR, whereas 12%, 5%, 2% and 1% harbor inner pairs in 5:3, 7:4, 7:5 and 8:5 MMRs, respectively. For $e_d = 0.1$, 12% hosts the pairs in 3:2 MMR, whereas 24% and 14% are captured in 4:3 and 7:5 MMRs.

Figure 6 shows the dynamical evolution for a typical case, which corresponds to two terrestrial planets in 7:4 MMR at the end of the simulation. The initial conditions and final locations are given in Table 2. As can be seen Figure 6, two migrating planets are temporarily trapped into 2:1 MMR at about 0.035 Myr, induced by a massive gas-giant of $10 M_J$ at 0.5 AU. However, the terrestrial planets simply remain at 2:1 MMR for a very short time. P_b and P_c will escape from 2:1 to 7:4 MMR because of strong perturbation from the giant planet, providing the evidence of

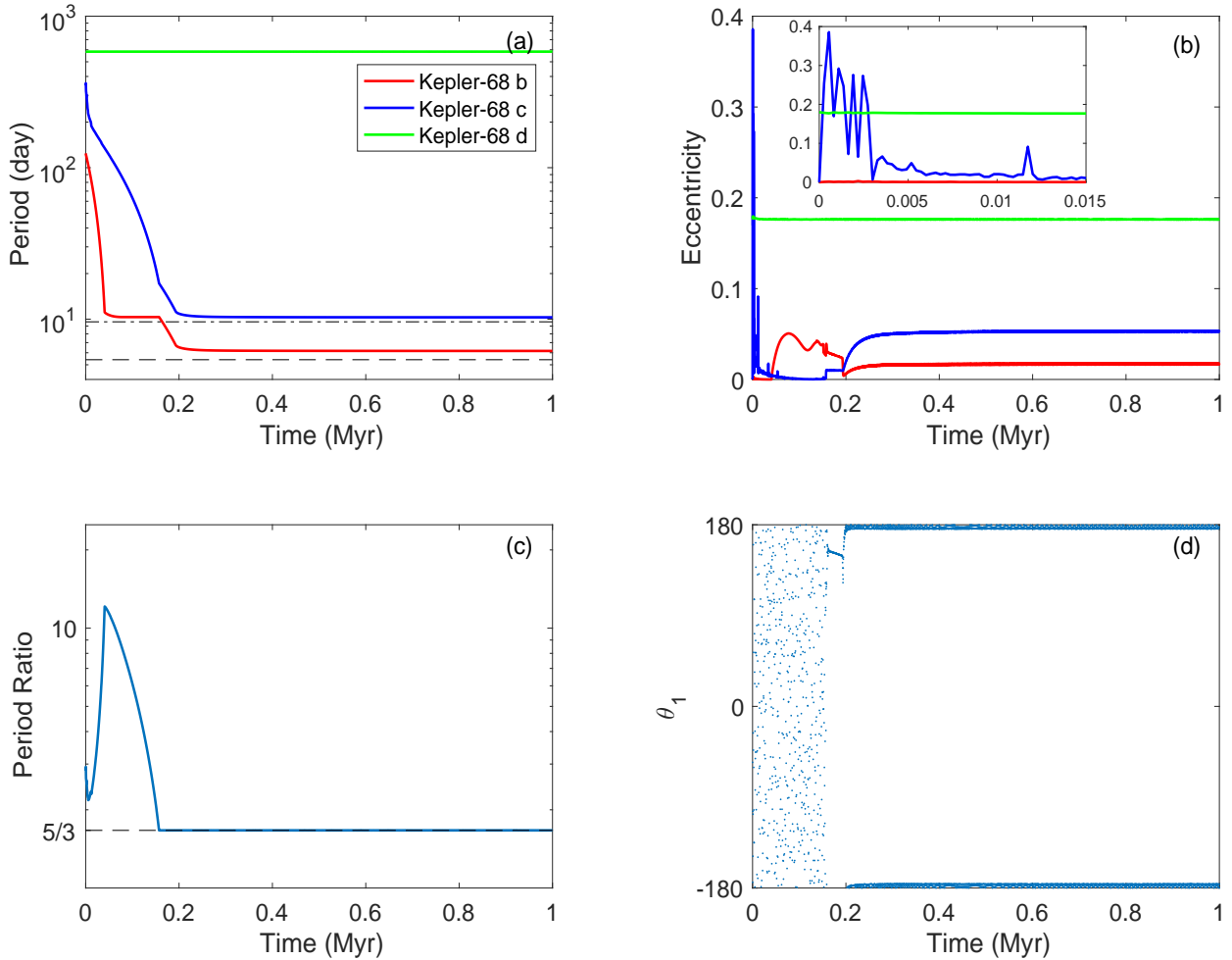


Figure 5. Orbital evolution of G2-4. The label of each panel and colored lines are the same as in Figure 2. A giant planet marked by green line locates at 1.4 AU with an initial eccentricity 0.18. Two inner terrestrial planets can be captured into 5:3 MMR at about 0.18 Myr. The resonant angle $\theta_1 = 3\lambda_1 - 5\lambda_2 + 2\varpi_1$ for 5:3 MMR librates about 180° with a tiny amplitude as shown in Panel (d).

formation of Kepler-68 system. In the subsequent evolution, the eccentricity of P_b could be stirred dramatically up to about 0.12 when two planets enter into MMR.

For the simulations in relation to a more massive giant planet, we find that the resultant configuration of the inner pair cannot be altered when the gas-giant revolves around the host star in a circular trajectory or move on an eccentric orbit of $e_d \leq 0.02$. However, in the case of the giant planet orbiting its central star with $e_d > 0.02$, the eccentricity of inner terrestrial especially the one closer to the giant planet will be excited to higher than 0.1 at least once. In some cases, the eccentricity of P_c can be excited to be about 0.4 for several times. Due to the eccentricity damping caused by the gas disk, the orbital migration will be speeded up. Meanwhile, the resonance web is dense for compact planetary systems (Namouni & Morais 2015). Thus, inner terrestrial planet pair have chance to be captured into high order MMRs. These outcomes favor formation scenario for two inner planets due to a distant gas-giant with an eccentric orbit.

3.3 Group 3: Secular Resonance

The gas disk inside the orbit of giant planet might have been seriously depleted by planetary or stellar accretion (Nagasawa et al. 2005) when terrestrial planets migrate to the region near its observed orbit. Then gaps are created around orbits of planets (Goldreich & Tremaine 1980; Takeuchi et al. 1996). The configuration of inner planet pair will be reshaped by secular perturbation stemming from the outermost companion and the gas disk exterior to planets.

The gravity of disk with an inner boundary at d ($d > a_d$) contributes to the planet i is given by the formula (Nagasawa et al. 2003)

$$\mathbf{f}_{i,disk} = 8\pi G \Sigma_g(r_i) \frac{\mathbf{r}_i}{r_i} \sum_{n=0} \left[B_n \left(\frac{r_i}{d} \right)^{2n+1/2} \right], \quad (6)$$

where

$$B_n \equiv \left[\frac{(2n)!}{2^{2n} (n!)^2} \right]^2 \frac{n}{(4n+1)}. \quad (7)$$

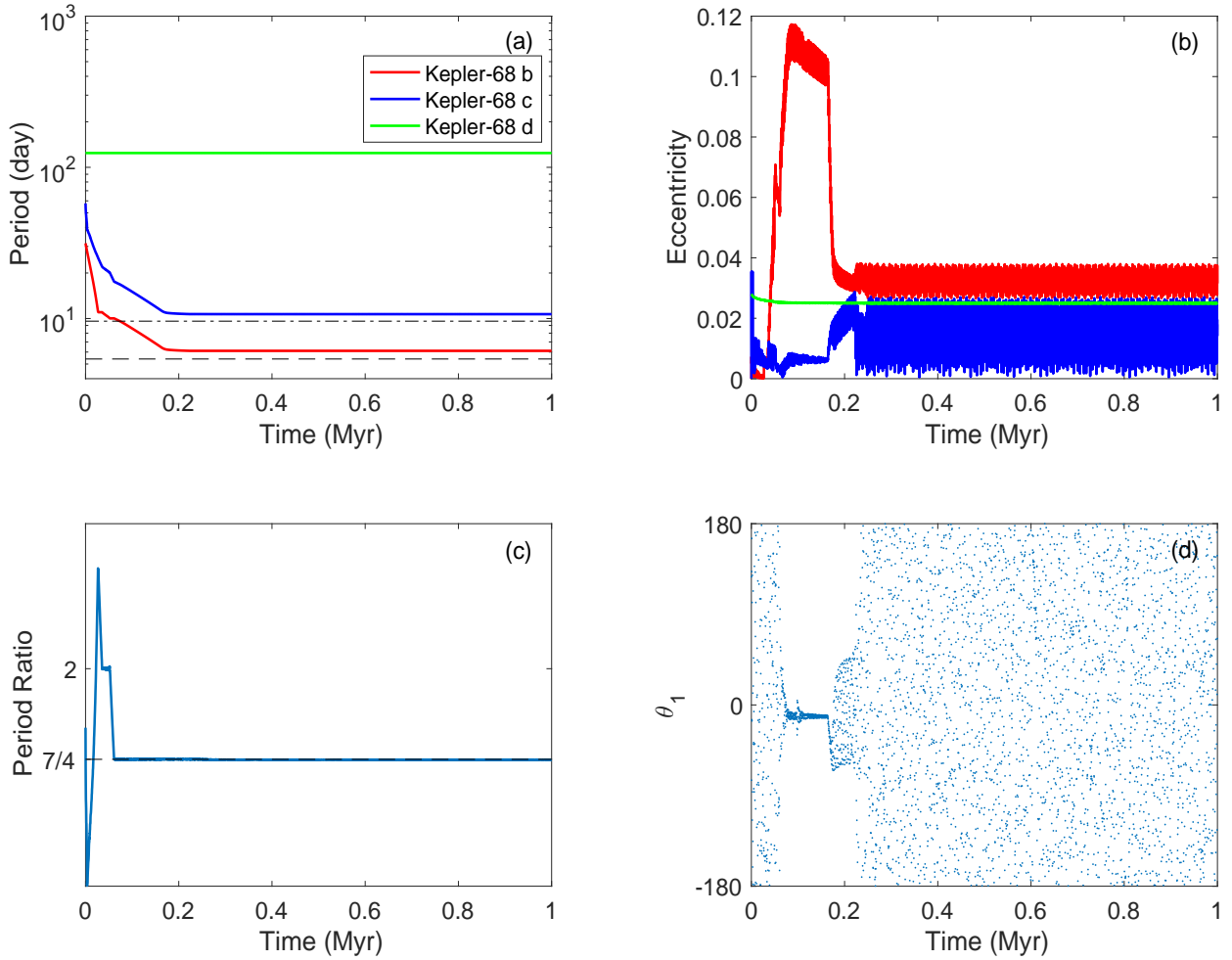


Figure 6. Same as in Figure 2, orbital evolution of G2-1 and G2-2. The initial locations of P_b , P_c and P_d are 0.2, 0.3 and 0.5 AU, respectively. Here e_d is 0.03. Note that P_b and P_c are temporarily trapped into 2:1 MMR at about 0.035 Myr, subsequently they have been involved in 7:4 MMR since 0.077 Myr along with a resonant angle $\theta_1 = 4\lambda_1 - 7\lambda_2 + 3\varpi_1$ tuning libration into circulation.

$\Sigma_g(r)$ refers to the same as in Equation (1). Here we set $d = 2$ AU. As a consequence, the eccentricity damping and type I migration caused by the gas disk on the planets disappear. The dissipation of disk can trigger secular perturbation between planets, thereby leading to angular momentum exchange and modifying their eccentricities (Nagasawa et al. 2003). The secular resonances occur only when the mass of outer disk is comparable to that of the giant planet (Nagasawa et al. 2005). The region of secular resonance gradually moves inward as gas density decreases. And we adopt an initial surface density of disk by Equation (1) with a disk depletion timescale $t_n = 10^6$ yr. According to the analysis of secular resonance (Heppenheimer 1980) and the disk model in this work, the location of secular resonance decreases from 0.8 AU to 0.02 AU which sweeps through the region of the terrestrial planets in the system.

Figure 7 shows the eccentricities of the inner planet pair (each colored by red and blue line) of Kepler-68 system evolve over a timescale of 1 Myr, resulting from secular

resonance by the giant planet with a variable mass. Here P_b and P_c are initially assumed to locate on circular orbits, and their masses and semi-major axes are listed in Table 1. Additionally, e_d corresponds to the observed value 0.18. The solid, dashed and dash-dotted lines represent the eccentricity evolution of P_b and P_c induced by the giant planet of a mass of 1, 5 and 10 M_J , respectively. As can be seen from Figure 7, we can see that the amplitude of eccentricity excitation of two terrestrial planets increases as the mass of gas-giant goes up. To be more specific, for $m_d = 1 M_J$, the simulations indicate that both of eccentricities are not well excited below 0.05. However, the eccentricities can be pumped up to 0.15 for $m_d = 5 M_J$, while they reach about 0.30 for $m_d = 10 M_J$.

As reported in Table 1, the eccentricity of P_c is not well confirmed. One of the orbital fittings indicates that e_b and e_c both are nearly zero (Gilliland et al. 2013; Mills et al. 2019), whereas an alternative orbital solution from observations show that e_c is approximately 0.42 (Van Eylen & Albrecht

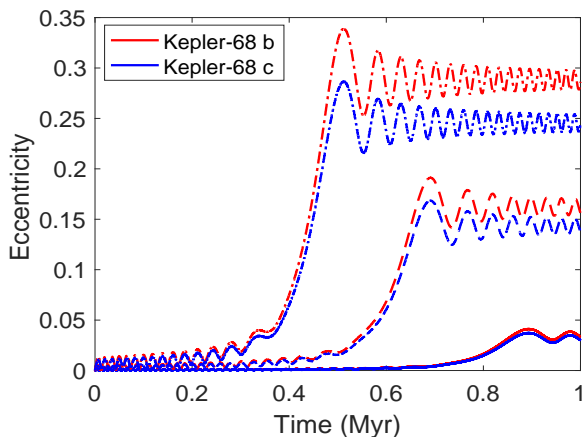


Figure 7. Eccentricity evolution of Kepler-68 b and Kepler-68 c (colored by red, blue) under secular resonance of the giant planet and disk. The solid, dashed and dash-dotted lines each represent the eccentricity evolution of the inner planet pair induced by a giant planet with a mass of 1, 5 and 10 M_J , respectively.

2015). According to our outcomes, e_c can be stirred up to above 0.2 only if m_d is more massive than 5 M_J . In such cases, e_b and e_c can be further excited in the evolution. On the other hand, as P_b moves much closer to the host star than P_c , thus the tidal effect by the central star plays a vital part in P_b , thereby resulting in the damping of eccentricity within $2.7 \times 10^5 Q'$ years, which seems to be much longer than the timescale of secular resonance as shown in Figure 7 (Mardling & Lin 2004; Zhou & Lin 2008). Here we suppose the density of terrestrial planet is about 3 g cm^{-3} , where Q' is the tidal dissipation factor. Hence we can estimate the timescale of eccentricity damping of P_c by tidal effect is approximately $6.6 \times 10^6 Q'$ years, implying that the eccentricity of P_c is difficult to be damped.

On the other hand, we note that the eccentricity of P_c is possibly excited to be above 0.2 when m_d is larger than 5 M_J . In contrast, P_c will stay at circular orbit with a less massive giant planet.

4 DISCUSSION AND CONCLUSION

In this work, we primarily conduct thousands of numerical simulations to explore the configuration formation for two inner terrestrial planets near MMRs as a result of the perturbation of the outermost gas-giant for the Kepler-68 system. Here we summarize the major outcomes and conclude that,

(i) For the system only harboring two terrestrial planets, they are inclined to be trapped into 2:1 or 3:2 MMRs, which depends on the speed of type I migration. When $0.3 \leq f_1 \leq 1$, the inner planet pair prefers to be captured into 3:2 MMR, whereas with a low speed of orbital migration $f_1 \leq 0.1$, the two terrestrial planets are more likely to be associated with 2:1 MMR. The results obtained here are consistent with those reported in our earlier work (Wang & Ji 2014).

(ii) For the system composed of two terrestrial planets and an outermost giant planet, we note that the inner planet pair can eventually reach similar configuration in the secular evolution like those for the two-planet system, when the

giant planet orbits the central star in a circular trajectory. As a comparison, for the three-planet system that one giant planet moves on eccentric orbit, we find that the terrestrial planets can be involved in 5:3 MMRs, being indicative of a close match with the currently observed orbits for Kepler-68. Further study shows that the inner pair would be captured in 7:4 or 8:5 MMRs if there is a more massive gas-giant at closer orbit in the system.

(iii) In view of the depletion of gas disk, the secular resonance may sweep up the nominal locations of inner terrestrial planets. Hence, the eccentricities of inner planets can be excited up to 0.2 with a massive giant planet of $m_d \geq 5 M_J$. Otherwise, the terrestrial planets retain to be circular orbits for a lower mass of the outermost companion.

Allowing for above-mentioned formation scenario, there are several critical factors that may have influence on resultant configuration of two terrestrial planets in the planetary system. First, the speed of orbital migration can play a significant role in shaping the final orbits of inner planet pair. With a faster orbital migration, the planet pair prefers to habitat in a more compact configuration (Hands & Alexander 2016). Second, the mass ratio, which is related to the speed of orbital migration, can further affect the near-resonant configuration for two terrestrial planets. To better understand this circumstance, here we perform 2000 additional simulations to investigate the systems by altering their initial masses in the range of 1 to 10 M_\oplus and the three angles. Figure 8 shows final configurations for two terrestrial planets in MMRs. In our simulations, we assume the planets originally locate at 0.2 and 0.3 AU, respectively. For $m_b/m_c < 1$, we observe that the two planets are inclined to be involved in 3:2 MMR. Based on the estimation of isolation mass (Ida & Lin 2004), the mass of solid core corresponds to the semi-major axis where they are formed with $m \propto a^{3/4}$. Accordingly, the mass of terrestrial planet grows up as its semi-major axis rises. If the system can maintain steady, the planet pair probably tends to be trapped in 3:2 MMR, e.g., K2-19 and Kepler-59 system (Petigura et al. 2020; Saad-Olivera et al. 2020). Otherwise, they are probably captured in 2:1 MMR. Third, the planet pair can be further trapped in high-order MMRs owing to the presence of a massive giant planet with an eccentric orbit. Additionally, the results are also related to the profile of the gas disks. With higher gas density, the speed of type I migration is higher. Planet pair is tend to be captured into 3:2 MMR rather than 2:1 MMR (Mustill & Wyatt 2011; Ogihara & Kobayashi 2013). With flatter gas disk, planets are more easier to be in 3:2 MMR (Wang & Ji 2017).

Moreover, we propose a likely scenario for configuration formation of the Kepler-68 system. As the eccentricity of P_c and the mass of P_d are not well determined (Gilliland et al. 2013; Van Eylen & Albrecht 2015; Mills et al. 2019), we infer that P_c cannot be stirred up to a moderate value unless there is a massive giant companion in the system. Future observations should be addressed to further decode the origin of Kepler-68. The innermost planet in this system is very close to the central star, the tidal effect arising from the central star is a main reason leading to the deviation from exact 5:3 MMR (Lee et al. 2013). Another possible scenario is the eccentricity damping effect induced by the depletion of the gas disk (Wang et al. in preparation).

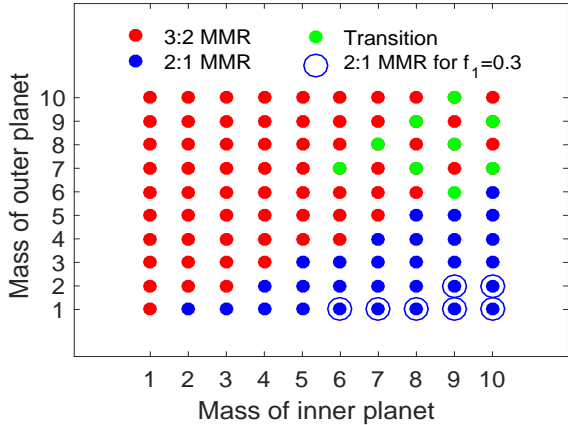


Figure 8. Final configuration related to MMRs for two planets with a mass ranging from 1 to 10 M_{\oplus} . Filled dots in red or blue represent the systems involved in 3:2 and 2:1 MMRs for $f_1 = 0.1$, respectively, while green dots stand for those of transition. Circles indicate those of 2:1 MMR for $f_1 = 0.3$.

Last but not least, our scenario can also be applied to formation of those systems that closely resemble Kepler-68, e.g., Kepler-65, Kepler-154 and Kepler-167 (Kipping et al. 2016; Berger et al. 2018; Mills et al. 2019). For instance, Kepler-65 harbors three inner terrestrial planets and a distant giant planet with an orbital period 258.8 day and an eccentricity 0.28, where two planet pairs among them are near 2.7 and 1.4, respectively (Chaplin et al. 2013). According to our formation scenario, we may infer that the eccentricities of three terrestrial planets can be stirred up to about 0.1 by the giant companion. During the subsequent migration, the outer planet pair could be trapped into 7:5 MMR, whereas the inner planet pair may be captured into 5:2 MMR as the outermost giant planet perturbs. Furthermore, as the innermost planet orbits close to the central star, its eccentricity may gradually decline by tidal effect from the host star over secular timescale as well as the decrease of semi-major axis, thereby producing the final period ratio between the inner pair above 2.5. In conclusion, our model can throw light on the formation of the planetary systems that harbor several terrestrial planets near MMRs inside and one giant planet outside as observed by Kepler mission.

ACKNOWLEDGEMENTS

We thank the anonymous referee for constructive comments and suggestions to improve the manuscript. This work is financially supported by the B-type Strategic Priority Program of the Chinese Academy of Sciences (Grant No. XDB41000000), the National Natural Science Foundation of China (Grant Nos. 11773081, 11573073, 11633009), CAS Interdisciplinary Innovation Team, Foundation of Minor Planets of the Purple Mountain Observatory and Youth Innovation Promotion Association.

DATA AVAILABILITY

The data underlying this article will be shared on reasonable request to the corresponding author.

REFERENCES

- Bae J., et al., 2019, *ApJL*, 884, L41
 Baruteau C., et al., 2014, *Protostars and Planets VI*, pp 667
 Batalha N. M., et al., 2013, *ApJS*, 204, 24
 Berger T. A., Huber D., Gaidos E., van Saders J. L., 2018, *ApJ*, 866, 99
 Bitsch B., Johansen A., Lambrechts M., Morbidelli A., 2015, *A&A*, 575, A28
 Bouvier, J., Matt, S. P., Mohanty, S., et al. 2014, *Protostars and Planets VI*, Henrik Beuther, Ralf S. Klessen, Cornelis P. Dullemond, and Thomas Henning (eds.), University of Arizona Press, Tucson, 433
 Chambers J. E., 1999, *MNRAS*, 304, 793
 Chaplin W. J., et al., 2013, *ApJ*, 766, 101
 Charalambous C., Martí J. G., Beaugé C., Ramos X. S., 2018, *MNRAS*, 477, 1414
 Chatterjee S., Tan J. C., 2014, *ApJ*, 780, 53
 Chiang E., Laughlin G., 2013, *MNRAS*, 431, 3444
 Cresswell P., Nelson R. P., 2006, *A&A*, 450, 833
 Duffell P. C., Haiman Z., MacFadyen A. I., D’Orazio D. J., Farris B. D., 2014, *ApJL*, 792, L10
 Dürmann C., Kley W., 2015, *A&A*, 574, A52
 Fabrycky D. C., et al., 2014, *ApJ*, 790, 146
 Ford E. B., Havlickova M., Rasio F. A., 2001, *Icar*, 150, 303
 Ford E. B., et al., 2012, *ApJ*, 750, 113
 Gilliland R. L., et al., 2013, *ApJ*, 766, 40
 Gillon M., et al., 2017, *Natur*, 542, 456
 Gladman B., 1993, *Icar*, 106, 247
 Goldreich P., Tremaine S., 1980, *ApJ*, 241, 425
 Gozdziewski, K., Migaszewski, C., Panichi, F., et al. 2016, *MNRAS*, 455, 104
 Granados Contreras A. P., Boley A. C., 2018, *AJ*, 155, 139
 Haisch K. E., Lada E. A., Lada C. J., 2001, *ApJL*, 553, L153
 Hands T. O., Alexander R. D., 2016, *MNRAS*, 456, 4121
 Hayashi C., 1981, *PThPS*, 70, 35
 Heppenheimer, T. A., 1980, *Icarus*, 41, 76
 Izidoro A., Ogihara M., Raymond S.N., et al. 2017, *MNRAS*, 470, 1750
 Ida S., Lin D. N. C., 2004, *ApJ*, 604, 388
 Kipping D. M., et al., 2016, *ApJ*, 820, 112
 Koenigl A., 1991, *ApJL*, 370, L39
 Kokubo E., Ida S., 1998, *Icar*, 131, 171
 Lambrechts M., Morbidelli A., Jacobson S. A., Johansen A., Bitsch B., Izidoro A., Raymond S. N., 2019, *A&A*, 627, A83
 Lee M. H., Peale S. J., 2002, *ApJ*, 567, 596
 Lee M. H., Fabrycky, D., & Lin D. N. C., 2013, *ApJ*, 774, 52L
 Lin D. N. C., Papaloizou J., 1986, *ApJ*, 309, 846
 Lithwick Y., Wu Y., 2012, *ApJL*, 756, L11
 Lissauer J. J., et al., 2011, *Natur*, 470, 53
 Lissauer J. J., et al., 2011, *ApJS*, 197, 8
 Liu B., Ormel C. W., 2017, *A&A*, 606, A66
 Liu B., Ormel C. W., 2018, *A&A*, 615, A138
 Liu B., Ormel C. W. & Johansen A., 2019, *A&A*, 624, A114
 Lykawka P. S., Ito T., 2013, *ApJ*, 773, 65
 Mandell A. M., Raymond S. N., Sigurdsson S., 2007, *ApJ*, 660, 823
 Marcy G. W., et al., 2014, *ApJS*, 210, 20
 Mardling R. A., Lin D. N. C., 2004, *ApJ*, 614, 955
 Marti, J. G., Giuppone, C. A., & Beauge, C. 2013, *MNRAS*, 433, 928

- Marti, J. G., Cincotta, P. M., & Beauge, C. 2016, MNRAS, 460, 1094
- McNally C. P., Nelson R. P., Paardekooper S.-J., 2019, MNRAS, 489, L17
- Mills S. M., et al., 2019, AJ, 157, 145
- Morton T. D., et al., 2016, ApJ, 822, 86
- Mustill A. J., Wyatt M. C., 2011, MNRAS, 413, 554
- Nagasawa M., Lin D. N. C., Ida S., 2003, ApJ, 586, 1374
- Nagasawa M., Lin D. N. C., Thommes E., 2005, ApJ, 635, 578
- Namouni F., Morais M. H. M., 2015, MNRAS, 446, 1998
- Ogihara M., Kobayashi H., 2013, ApJ, 775, 34
- Ogihara M., Morbidelli A., Guillot T., 2015, A&A, 578, A36
- Ogihara M., Kokubo E., Suzuki T. K., et al. 2018, A&A, 615, 63
- Paardekooper S.-J., Rein H., Kley W., 2013, MNRAS, 434, 3018
- Papaloizou J. C. B., Larwood J. D., 2000, MNRAS, 315, 823
- Petigura E. A., et al., 2020, AJ, 159, 2
- Raymond S. N., Mandell A. M., Sigurdsson S., 2006, Sci, 313, 1413
- Raymond S. N., Boulet T., Izidoro A., Esteves L., Bitsch B., 2018, MNRAS, 479, L81
- Rein H., 2012, MNRAS, 427, L21
- Robertson P., et al., 2012, ApJ, 754, 50
- Rowe J. F., et al., 2014, ApJ, 784, 45
- Saad-Oliveira X., Martinez C. F., Costa de Souza A., Roig F., Nesvorný D., 2020, MNRAS, 491, 5238
- Stassun K. G., Collins K. A., Gaudi B. S., 2017, AJ, 153, 136
- Sun Z., Ji J., Wang S., Jin S., 2017, MNRAS, 467, 619
- Suzuki T. K., Ogihara M., Morbidelli A., Crida A., Guillot T., 2016, A&A, 596, A74
- Takeuchi T., Miyama S. M., Lin D. N. C., 1996, ApJ, 460, 832
- Tanaka H., Takeuchi T., Ward W. R., 2002, ApJ, 565, 1257
- Terquem C., Papaloizou J. C. B., 2007, ApJ, 654, 1110
- Uehara S., Kawahara H., Masuda K., Yamada S., Aizawa M., 2016, ApJ, 822, 2
- Van Eylen V., Albrecht S., 2015, ApJ, 808, 126
- Wang S., Ji J., Zhou J.-L., 2012, ApJ, 753, 170
- Wang S., Ji J., 2014, ApJ, 795, 85
- Wang S., Ji J., 2017, AJ, 154, 236
- Ward W. R., 1997, Icar, 126, 261
- Wittenmyer R. A., et al., 2016, ApJ, 818, 35
- Zhou J.-L., Aarseth S. J., Lin D. N. C., Nagasawa M., 2005, ApJL, 631, L85
- Zhou J.-L., Lin D. N. C., Sun Y. S., 2007, ApJ, 666, 423
- Zhou J.-L., Lin D. N. C., 2008, IAUS, 285, IAUS..249

This paper has been typeset from a $\text{\TeX}/\text{\LaTeX}$ file prepared by the author.